STATUS UPDATE FOR THE HIGH GAIN HIGH EFFICIENCY TESSA-266 EXPERIMENT

Youna Park, Pietro Musumeci, Paul Denham, David Dang, Nick Sudar, UCLA, Los Angeles, USA
Alexander Zholents, Yine Sun, ANL, Argonne, USA
Tara Campese, Ivan Gadjev, Ronald Agustsson, Alex Murokh, RadiaBeam, Los Angeles, USA
Stephen Webb, Chris Hall, RadiaSoft, Boulder, USA

Abstract

This paper will provide a status report on the high gain high efficiency TESSA-266 experiment planned at the Linac Extension Area (LEA) facility at Argonne Photon Source (APS). The goal of this project which is carried forward by a multi-institutional collaboration between university (UCLA), national laboratory (ANL) and small industries (Radiabeam and Radiasoft) is to demonstrate very high efficiency electron beam energy extraction in a 4-meter long strongly tapered helical undulator seeded by an ultraviolet 1 GW peak power laser seed pulse, and to study the spatial and spectral properties of the amplified radiation. We focus here on the discussion of the break-section area in between the undulators which has been designed to maximize the efficiency, and show the results of the numerical simulations for the system.

INTRODUCTION

Free-Electron-Lasers enjoy many unique properties as radiation sources, including high power, coherence and tunability and have been at the forefront of scientific research for decades. Especially in the short wavelength region of the electromagnetic spectrum, FELs have enabled a novel generation of radiation sources opening new frontiers in scientific research. On the other hand a characteristic drawback for conventional Free-Electron-Lasers amplifiers is that the energy efficiency is actually relatively poor, limited by the Pierce parameter [1] which at short wavelength (ultraviolet and below) is typically below 1 percent and often below 0.1 percent.

Following up earlier work on Inverse Free Electron Laser acceleration [2], few years ago a novel regime of operation has been proposed to greatly increase the FEL efficiency using prebunched electron beams, intense seed laser, and strongly tapered undulators (so called TESSA scheme) [3]. An experimental demonstration of the TESSA concept in the mid-infrared was carried out at BNL [4] where using a 200 GW seed laser at 10 μm wavelength, an energy extraction efficiency as high as 30 % was demonstrated. The intense seed laser pulse used for this experiment hindered measurements of the spatial and spectral properties of the newly generated radiation (i.e. the experiment was carried out in the low-gain TESSA regime).

The current TESSA-266 project aims at pushing the performances of the proof-of-principle BNL experiment and explore this interaction in the high gain regime (using a less intense seed laser pulse) and extending the scheme to shorter wavelengths where high efficiency radiation sources would be extremely attractive (EUVL). The experimental design is based on a tapered gap-tunable helical Halbach [5] undulator which will be installed in the Linac Extension Area (LEA) at the end of the Argonne Photon Source injection linac. The APS linac will provide 375 MeV and up to 1 kA e-beam at 1-10 Hz pulse repetition rate in the interleaving mode that makes the beam available for this experiment 75 % of time. A seed laser of 1 GW and pulse length 0.6 ps will then be used first to bunch, extract energy and quickly decelerate the electron beam, yielding high gain TESSA amplification and an extraction efficiency which in the ideal simulation case reaches values as high as 10 percent (see Table 1 for a summary of the experiment parameters).

EXPERIMENT DESIGN

The tapered helical undulator for TESSA-266 is designed to maintain the resonant condition as the electrons lose their energy to the radiation along the interaction varying the undulator K factor while keeping the undulator period constant [6]:

$$\gamma_r^2 = \frac{\lambda_u}{2\lambda}(1 + K^2) \qquad (1)$$

where λ_u is the undulator period, λ is the laser wavelength, and K the normalized undulator vector potential.

The undulator period is chosen to be at 3.2 cm in order to satisfy the resonance condition with e-beam energy of 375 MeV and wavelength of 266 nm with a gap of sufficient size to hose the vacuum pipe (> 5.5 mm).

Table 1: TESSA266 Nominal Parameters

Element	
Beam Energy	375 MeV
Peak Current	1 kA
Emittance	2 um
Energy Spread	0.1 %
RMS Mean Spot Size	47 um
Undulator Period	32 mm
Undulator K Parameters	2.8 - 2.4
Radiation wavelength	266 nm
Seed Power	1 GW

A number of considerations entered the final choice on the length of the undulator sections in the design of the experiment. There is enough space in the LEA tunnel to house
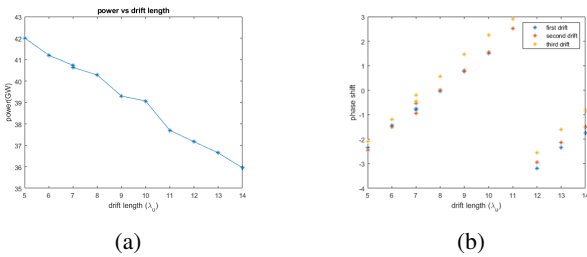
(a)   (b)

Figure 1: Optimized power output of time-independent simulation obtained from parameters in Table 2. (a) Output power vs. Drift length. A linear fit indicates that increasing the drift length of the break-sections, the output power decreases by around .5 % per centimeter, (b) Optimized phase shift vs. drift length in each break section.

a very long undulator, but it has been shown that high gradient deceleration is particularly important in order to avoid excessive growth of the synchrotron side-band instability which is the main limit to the radiation extraction efficiency. In order to leave open the possibility to reach the ambitious goal of 10 % efficiency we then set the undulator length to 4 m. A compromise is then made between i) using one long undulator which would enable continuous energy exchange and ii) breaking up the interaction using multiple undulator sections. The latter option leaves the opportunity to add focusing elements that can squeeze the beam transversely and maximize energy extraction efficiency [7]. In addition, a maximum undulator section length of 1 m is set by the length of the mill workplane at Radiabeam where the undulator is going to be built. In the final design of the experiment the THESEUS (Tapered HElical SEgmented Undulator System) undulator will comprise four 990 mm long sections.

An integral part of the THESEUS design are the break-sections in between the undulators. The radiation in these regions freely diffracts quickly reducing the on-axis intensity at the restart of the interaction and degrading the energy exchange. With our parameters we simulated that the output power would decrease as much as 0.5% per centimeter of break section length (Figure 1a) putting a strong request on keeping the break sections as short as possible.

At the same time, a large number of elements needs to fit within this section, transforming the design of this part of the experiment in a unique engineering feat. The focusing schemes for TESSA266 includes a doublet of permanent magnet quadrupoles to minimize the e-beam size along the interaction. [8]. Furthermore, simulations indicate that a tunable phase shifter would be highly beneficial in order to maximize the energy extraction. Vacuum pumps, undulator and laser diagnostic station add their own level of complexity to the challenge. The final design includes an extremely dense 17 cm long break section, hosting doublet quadrupoles, a phase shifter, a diagnostic station, and built-in bellows for correcting misalignments as shown in Figure 2.

Using Genesis simulations, we determined that the optimal phase shift in this configuration will be close to a full 2π
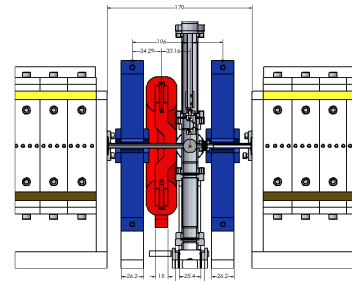

Figure 2: Break Section Design with the two permanent quadrupoles (blue), electromagnetic dipole (red), and diagnostic station (grey).

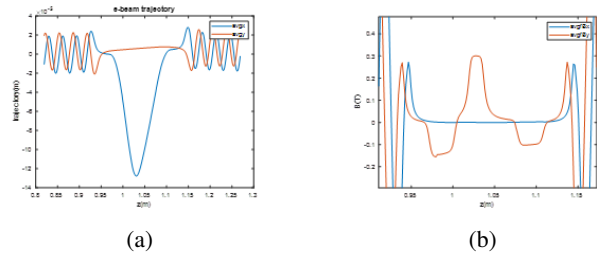(a)   (b)

Figure 3: GPT Simulation of the break section with two transversely shifted quadrupoles and an electromagnetic dipole. (a) e-beam trajectory (b) magnetic field.

shift (Figure 1b). To obtain a phase-shifter in the very limited space available, we took advantage of the quadrupole pair already included in the focusing lattice. When a quadrupole is shifted in the transverse direction it behaves as a dipole and can be used to deflect the beam. The phase shift is then based on the use of remotely controllable translation stages for the PMQs (which effectively double as dipoles for this) and the addition of a small electromagnetic dipole (EMD) in between, to form a very short 3-dipole mini-chicane (Figure 3b). The chicane lengthens e-beam trajectory (Figure 3a) so that the phase of the electron beam micro-bunches is shifted relative to the photons that travels in a straight trajectory.

The transverse shift in the quadrupole position required to correct the trajectory for a given dipole field is:

$$\Delta x_{1,2} = \frac{L_D B_D}{L_Q g_Q} \frac{z_{2,1}}{z_1 + z_2} \qquad (2)$$

where L_D and B_D are the length and field strength of the EMD respectively, L_Q and g_Q are the length and gradient of quadrupole, z_1 and z_2 the center-to-center displacements from each quadrupole to the EMD. The shift would then be minimized if the dipole was placed in the center of the break section equidistant from the two quadrupoles. However because of the diagnostic cross, it is not feasible to place the EMD in the center. In addition, due to the very tight boundaries around the diagnostic station and the quadrupoles, only 28-mm space in the longitudinal direction and 38-mm transverse was available for the dipole. This required maximizing the coil volume and bending the pole to redirect the field
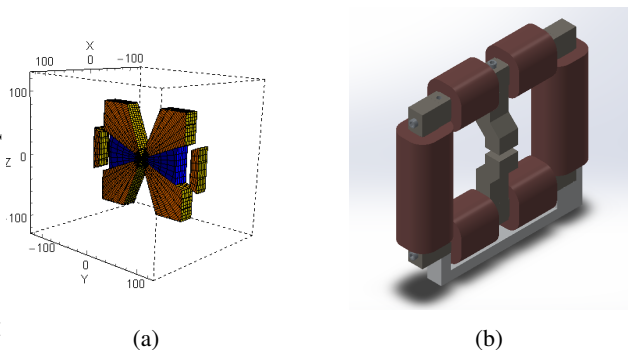
THP073

(a) (b)

Figure 4: Phase shifter element design. (a) Adjustable hybrid quadrupole design, (b) H-shaped electromagnetic dipole with peeking out pole.

toward the center of the assembly (Figure 4b). A novel adjustable hybrid permanent-magnet-based quadrupole design (Figure 4a) was developed in order to enable tuning of the quadrupole gradient and minimize the e-beam size inside the undulators. The hybrid quadrupole design is based on two permanent magnets, four steel poles and two steel shims. The shims can be moved from 5 mm to 15 mm which changes the integrated quadrupole gradient from 6.5 T to 7 T by redirecting the magnetic flux.

GPT simulations of the beam trajectory show that a full phase shift can be achieved without increasing the drift length or compromising the quadrupole focusing (Figure 5). In the plot one can see that for a full phase shift the quadrupoles is shifted by less than .5 mm from the on-axis position and the EMD field will be at around .25 T which is well below 0.5 T saturation field for this magnet.
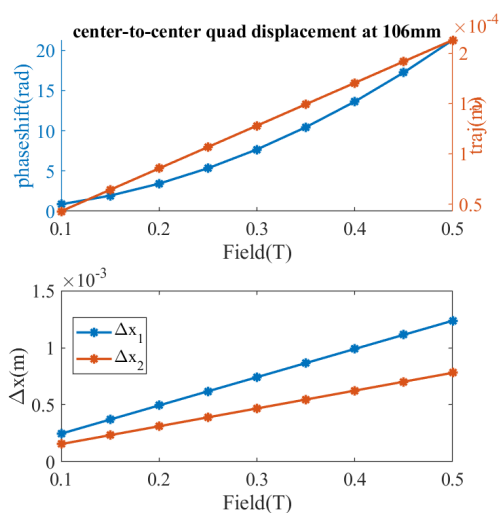

Figure 5: phase shift and quadrupole shift vs. dipole magnetic field strength. For a full phase shift the dipole field is 0.25 T, for which the first quadrupole needs to be shifted by 0.7 mm to straighten the electron trajectory.
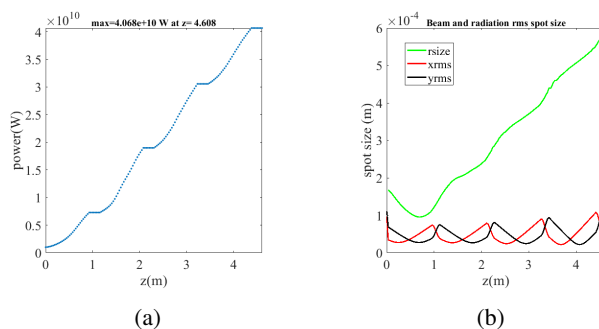

(a) (b)

Figure 6: FEL Time-Independent Genesis Simulation Result. (a) radiation power at the end of the 4th undulator, (b) radiation (green) and e-beam size (red and black).

SIMULATION RESULTS

The optimal tapering for the experiment is finally determined using a period-by-period Genesis simulation as discussed in [3]

$$\frac{dK}{dz} = -2k_u K_l \sin\psi_r \tag{3}$$

where k_u is the undulator wavenumber, K_l is the normalized laser vector potential and ψ_r the design resonant phase.

The time-independent simulation result for four undulator sections of 29 undulator periods, the nominal drift length, and quadrupoles of 195 T/m gradient, along with optimal phase shifts in between undulator sections shows an extraction efficiency near ten percent (Figure 6).

Table 2: TESSA266 Distances

Element	Physical Length
THESEUS section length	989.4 mm
Physical break section length	170 mm
Total Sys. Length with pre-buncher	6610 mm
Quadrupole Effective Length	26.2 mm
EMD Effective Length	15.0 mm

ACKNOWLEDGEMENT

REFERENCES

[1] C. Pellegrini, A. Marinelli, and S. Reiche, "The physics of x-ray free-electron lasers," *Rev. Mod. Phys.*, vol. 88, p. 015006, Mar 2016. doi:10.1103/RevModPhys.88.015006

[2] J. Duris, P. Musumeci, and R. Li, "Inverse free electron laser accelerator for advanced light sources," *Physical Review Special Topics-Accelerators and Beams*, vol. 15, no. 6, p. 061301, 2012. doi:10.1103/PhysRevSTAB.15.061301

[3] J. Duris, A. Murokh, and P. Musumeci, "Tapering enhanced stimulated superradiant amplification," *New Journal of Physics*, vol. 17, no. 6, p. 063036. doi:10.1088/1367-2630/17/6/063036

[4] N. Sudar, P. Musumeci, J. Duris, I. Gadjev, M. Polyanskiy, I. Pogorelsky, M. Fedurin, C. Swinson, K. Kusche, M. Babzien, and A. Gover, "High efficiency energy extraction from a relativistic electron beam in a strongly tapered undulator," *Phys. Rev. Lett.*, vol. 117, p. 174801, Oct 2016. `doi:10.1103/PhysRevLett.117.174801`

[5] K. Halbach, "Physical and optical properties of rare earth cobalt magnets," *Nuclear Instruments and Methods in Physics Research*, vol. 187, no. 1, pp. 109 – 117, 1981. `doi:10.1016/0029-554X(81)90477-8`

[6] N. Kroll, P. Morton, and M. Rosenbluth, "Free-electron lasers with variable parameter wigglers," *IEEE Journal of Quantum Electronics*, vol. 17, pp. 1436–1468, August 1981. `doi:10.1109/JQE.1981.1071285`

[7] C. Emma, K. Fang, J. Wu, and C. Pellegrini, "High efficiency, multiterawatt x-ray free electron lasers," *Phys. Rev. Accel. Beams*, vol. 19, no. 2, p. 020705, 2016. `doi:10.1103/PhysRevAccelBeams.19.020705`

[8] Y. Park, P. Musumeci, N. Sudar, A. Zholents, A. Murokh, Y. Sun, S. Webb, C. Hall, and D. Bruhwiler, "Strongly Tapered Undulator Design for High Efficiency and High Gain Amplification at 266 nm," in *Proc. FEL'17*, Santa Fe, NM, USA, Aug. 2017, pp. 49–52. `doi:10.18429/JACoW-FEL2017-MOP011`